The Effect Of Convolution Code Structural Property To Reduce The Bit Error Rate In Underwater Acoustic Channel

N.R.Krishnamoorthy, Immanuel Rajkumar, Jerry Alexander, Archanadevi, Abirami

Abstract: Data communication in underwater channel is most challenge task for an ocean researchers. The channel gives least error rate compared to space communication due to the various factors like high attenuation, heavy multipath propagation and dependence of low frequency signal. This limits the low bandwidth and short range communication. To overcome this, structure of the convolution encoder needs to be analyzed thoroughly for better error rate control for an underwater channel. In this paper structure property of convolution encoder with the code rate of ½ is analyzed. It is evident from the analysis that polynomial with least hamming distance and less code weight gives better efficiency than other polynomial.

Index Terms: Coding Gain, Hamming Distance, Convolution Code, Encoder Polynomial, Feed-Forward Encoder, Code rate.

1. INTRODUCTION

Underwtaer Acoustic Channel (UAC) is the one of most difficult channel for data transmission. It limits the bandwidth with an increase in both frequency and range [1]. For example, short ranges communication in the order of 100 meters will have the bandwidth of around 2.6 kHz, whereas a long range communication of 10 km is limited to the bandwidth of 100 Hz. Depending on the position of transmitter and receiver in UAC channel, the signal undergoes multipath propagation inside the channel with limited bandwidth. It is tedious task for the researchers to combat the signal degradation caused by this multipath propagation and to achieve a high data rate in the medium and long range communication. Another important factor to be considered is the Overlapping of symbol. For UAC, this increases to several hundreds of symbols. The two basic mechanisms in the formation of multipath spreads are ray bending and reflection. This mechanism purely depends on the channel geometry and the frequency of a transmitted signals. To predict the configuration of multipath and suppress the effect of it in UAC channel, a proper modeling of propagation model is essential. Few of available methods are theory of normal modes [2], Ray Tracing [3], Stochastic model [4] and Rayleigh fading Model [5]. Ray Tracing and theory of normal mode are the basis of propagation modeling. It is used to determine the coarse multipath structure. The various parameters that are used in the underwater communication channel are Attenuation Noise, Multipath effects, Doppler Shift, Surface Loss, Bottom Loss and Transmission Loss are as follows. There are various coding techniques are available for the underwater data communication such as convolution code, OFDM techniques, Adaptive Equalizer and Low Density Parity Check Code. In [6], the performance of the UAC channel is studied using Recursive Systematic Convolution (RSC) codes with random inter-leaver. Extrinsic Information Transfer Chart (EXIT) [7] analysis was performed using convolution code with generator polynomial (23, 35). In this, data is modulated by BPSK with PN training sequence. Doppler shift of the channel is estimated by adaptive algorithm along with BCH (64, 10) code [8]. In [9], the performance of convolutional code was studied by varying the power level and modulation levels. OFDM techniques without any Guard Interval [10] is applied to evaluate the performance of the channel. In this method Doppler scaling factors are interpolated using cubic B-splines and transformed it to the coefficient of the equalizer in the time domain. For coherent underwater acoustic communication, the performance of SC-FDE [11] is studied. In a conventional OFDM, IFFT is performed in the transmitting section and FFT in the receiving section. In [12], authors have applied the linear detector with MMSE optimization to avoid the effects of the interference caused by the Doppler distortion. Along with OFDM, IDMA technique [13] is applied to remove the multi-access interference in the UAC channel. This method makes use of the serial input serial output (SISO) decoder and Elementary Signal Estimator (ESE) in the receiver section. For a doubly spread channel, the multipath profile of the channel is measured using Orthogonal Signal Division Multiplexing (OSDM) [14] without an interpolation process. PN sequence based equalizer is designed for the shallow water communication. In this, a least square technique [15] and low order DFE [16] are used for the channel estimation for single carrier spread spectrum sequence. For MIMO acoustic communication, DFE [17], [18], Normalized Least Mean Square algorithm [19] and gradient-based LMS algorithm [20] is applied along with the turbo equalizer for the symbol estimation. In [21], authors applied bitwise inter-leaver of LDPC-OFDM encoding and showed that the error rate decreases as the number of OFDM subcarrier increases. For MIMO UAC system, a double layer detection scheme [22] is applied. In this paper, structure property of convolutional code is analyzed for the code rate of ½ with constraint length of 2 and 3. The simulation result evident that the polynomial with least hamming code and less code weight yields better bit error rate compared to other polynomial.

2 ENCODER WITH CONSTRAINT LENGTH OF 2

Encoding of data can be done in two ways such as Feedback encoder and Feed-Forward encoder. In the case of Feedback encoder, portion of output data is feed back to the input and coding is done. This leads to the complexity of the circuit and retrieval of data in the receiver section will be a complex. To avoid such a complexity, researchers will make use of feed forward encoder. In general Feed-Forward encoder provides better performance in terms of bit error rate compared to the Feedback encoder. To balance the performance of the encoder with less circuit complexity, the structural property of the Feed-Forward encoder is studied in detail to attain the better Error rate compared to the Feedback encoder.

The convolution encoder is represented by (v, u, m) where u and v represents the number of input and output terminal respectively and m is the number of memory elements. The encoder shown in figure 1 will be represented as (2, 1, 2) encoder with the constraint length of 3. The outputs v can be taken at different positions. Depending on the position, we will get different polynomial. For example as shown in the figure 1, the output V1 is taken from input and after the second delay with its binary representation as 101. Similarly the output V2 is taken from input, after first and second delay. Therefore it is represented as 111 in the binary form. Combining the V1 and V2, the polynomial representation of the encoder shown in the figure 1 is given as [5, 7]. The figure 2 is the Feed-Forward encoder with the polynomial [1, 5]

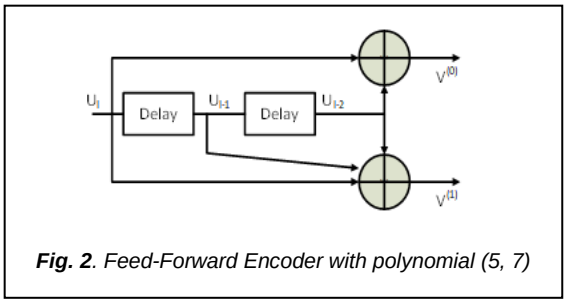

***Fig. 2**. Feed-Forward Encoder with polynomial (5, 7)*

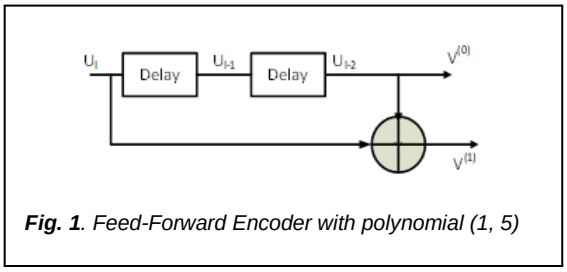

***Fig. 1**. Feed-Forward Encoder with polynomial (1, 5)*

The state table for the polynomial [1, 5] and [5, 7] is listed in the Table 1. It elaborates the behavior of the polynomial for encoding the message data. From the Table 1, state diagram and modified state diagram is obtained and it is shown in the Figure 3 to 6. Table 2 lists out the parameter required for the computation of the WEF function for the polynomial [1, 5]. It is obtained from the modified state diagram shown in the Figure 4. The minimum hamming distance and coding gain is evaluated as 5 and 3.98 dB.

TABLE 1
STATE TABLE FOR AN (2, 1, 3) ENCODER FOR CONSTRAINT LENGTH OF 3

Input	Present state	Next State	Output V_0 V_1 for Polynomial [1, 5]	[5, 7]
0	00 (S_0)	00 (S_0)	00	00
0	01 (S_2)	00 (S_0)	11	11
0	10 (S_1)	01 (S_2)	00	01
0	11 (S_3)	01 (S_2)	11	10
1	00 (S_0)	10 (S_1)	01	11
1	01 (S_2)	10 (S_1)	10	00
1	10 (S_1)	11 (S_3)	01	10
1	11 (S_3)	11 (S_3)	10	01

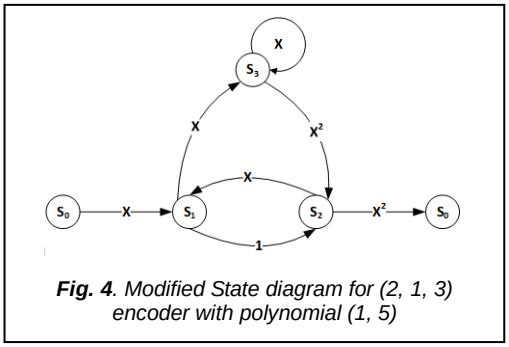

***Fig. 4**. Modified State diagram for (2, 1, 3) encoder with polynomial (1, 5)*

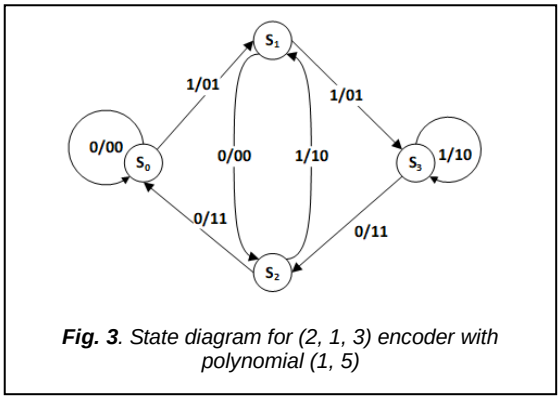

***Fig. 3**. State diagram for (2, 1, 3) encoder with polynomial (1, 5)*

In the similar manner, the structure property for the polynomial [5, 7] is computed and it is elaborate in the detail in the Figure 5 and 6 and Table 3.

TABLE 2
CYCLE AND FORWARD PATH FOR AN (2, 1, 3) ENCODER WITH THE POLYNOMIAL [1, 5]

Cycles			Cij		Forward Path			
Label	Path	Gain	Label	Gain	Label	Path	Gain	Delta(Δ)
C1	S_3 S_3	X	C2, C3	X^2	FP1	S_0 S_1 S_2 S_0	X^5	1 - X
C2	S_1 S_2 S_1	X			FP2	S_0 S_1 S_3 S_2 S_0	X^6	1
C3	S_1 S_3 S_2 S_1	X^2						

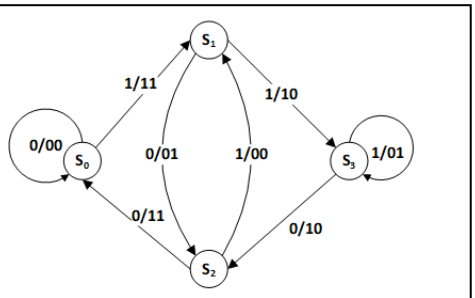

***Fig. 5**. State diagram for (2, 1, 3) encoder with polynomial (5, 7)*

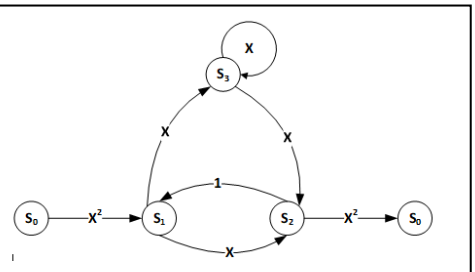

***Fig. 6**. Modified State diagram for (2, 1, 3) encoder with polynomial (5, 7)*

The Weight Enumerated Function (WEF) A(X) of a graph is computed using Mason's formula as

TABLE 3
CYCLE AND FORWARD PATH FOR AN (2, 1, 3) ENCODER WITH THE POLYNOMIAL [5, 7]

Cycles			C_{ii}		Forward Path			
Label	Path	Gain	Label	Gain	Label	Path	Gain	Delta(Δ)
C1	$S_3 S_3$	X	C2, C3	X^4	FP1	$S_0 S_1 S_2 S_0$	X^5	$1-X$
C2	$S_1 S_2 S_1$	X^3			FP2	$S_0 S_1 S_3 S_2 S_0$	X^4	1
C3	$S_1 S_3 S_2 S_1$	X^2						

$$A(X) = \frac{\sum_i F_i \Delta_i}{\Delta} \quad (1)$$

Where

$$\Delta = 1 - \sum_i C_i + \sum_{i',j'} C_i' C_j^i - \sum_{i'',j'',k''} C_i'' C_j'' C_k'' + ... \quad (2)$$

$\sum_i C_i$ – Sum of Cycle gains

$\sum_{i',j'} C_i' C_j^i$ - Product of cycle sum of non – touching cycles F

Fi – gain of the i^{th} forward path

Δi – Δ correspond to the i^{th} forward path

For the polynomial [1, 5] the delta values is given below

$$\Delta = 1 - (C1 + C2 + C3) + (C2 * C3) = 1 - 2X \quad (3)$$

Substituting the delta and forward path gain for the polynomial [1, 5] in the equation 1, WEF results as below

$$A(X) = \frac{X^5}{1-2X} = X^5 + X^6 + ... \quad (4)$$

Free Hamming Distance (dfree) is the lowest order of the WEF function and its corresponding amplitude is the gain of the dfree (Adfree). For the polynomial [1, 5] it is observed that these values are 5 and 1 and it is listed below.

dfree = 5, Adfree = 1 and

The Coding gain for the given polynomial is given by the equation (5)

$$\gamma = 10\log_{10}(R \times d_{free}) \quad (5)$$

For the polynomial [1, 5], the coding gain is obtained by substituting the code rate (R) and the dfree values in the equation 5 as below

$$\gamma = 10\log_{10}(R \times d_{free})$$
$$= 10\log_{10}(5/2)$$
$$= 3.98\,\text{dB}$$

For the polynomial [5, 7] the delta values is given below

$$\Delta = 1 - (C1 + C2 + C3) + (C2 * C3) = 1 - X - X^2 - X^3 + X^4 \quad (6)$$

Substituting delta and forward path gain in the equation 1 results as below

$$A(X) = \frac{X^5 - X^6 + X^4}{1 - X - X^2 - X^3 + X^4} = X^4 + 2X^5 + ... \quad (7)$$

dfree = 4, Adfree = 1 and

$$\gamma = 10\log_{10}(R \times d_{free})$$
$$= 10\log_{10}(4/2)$$
$$= 3.01\ \text{dB}$$

3 ENCODER WITH CONSTRAINT LENGTH OF 3

In this section, structure property of Feed-Forward encoder with constraint length of 3 is discussed. Figure 7 and 8 shows the FeedForward Encoder with the polynomial of (10, 11) and (13, 17). The operation of a convolutional encoder is described by a state table as shown in Table 4. The state of an encoder s defined with respect to its shift register contents. For an encoder, the i^{th} shift register at time unit l, contains vi bits.

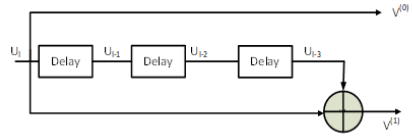

Fig. 7. Feed-Forward Encoder with Polynomial (10, 11)

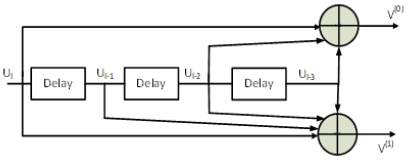

***Fig. 8**. Feed-Forward Encoder with Polynomial (13, 17)*

For an (2, 1, 3) encoder, the next state is 110 for an input of 1 corresponds to the present state of 101. The output for this state is 01. The Table 4 lists out the operation of encoder (2, 1, 3) encoder for the codeword polynomial (13, 17).

The state assignment is as follows
{000, 001, 010, 011, 100, 101, 110, 111} as
{S0, S4, S2, S6, S1, S5, S3, S7}

From the state Table 4, state diagram can be drawn. For instance, for the state S0, if the input is 0, the encoder remains in the same state with the output of and it goes to the state S1 for the input of 1 with the output value of.

Similar way, the other state from S1 to S7 is elaborated and it is shown in the Figure 9. To illustrate the structure property of convolution code, the state diagram shown in figure1 is redrawn as Figure 10. In the modified state diagram, the state output are described in terms of Hamming weight as 1, X or X2.

TABLE 4
STATE TABLE FOR AN (2, 1, 3) ENCODER FOR CONSTRAINT LENGTH OF 4

Input	Present State	Next State	Output V_0V_1 for polynomial	
			[10, 11]	[13, 17]
0	000 (S_0)	000 (S_0)	00	00
0	001 (S_4)	000 (S_0)	01	11
0	010 (S_2)	001 (S_4)	00	11
0	011 (S_6)	001 (S_4)	01	00
0	100 (S_1)	010 (S_2)	00	01
0	101 (S_5)	010 (S_2)	01	10
0	110 (S_3)	011 (S_6)	00	10
0	111 (S_7)	011 (S_6)	01	01
1	000 (S_0)	100 (S_1)	11	11
1	001 (S_4)	100 (S_1)	10	00
1	010 (S_2)	101 (S_5)	11	00
1	011 (S_6)	101 (S_5)	10	11
1	100 (S_1)	110 (S_3)	11	10
1	101 (S_5)	110 (S_3)	10	01
1	110 (S_3)	111 (S_7)	11	01
1	111 (S_7)	111 (S_7)	10	10

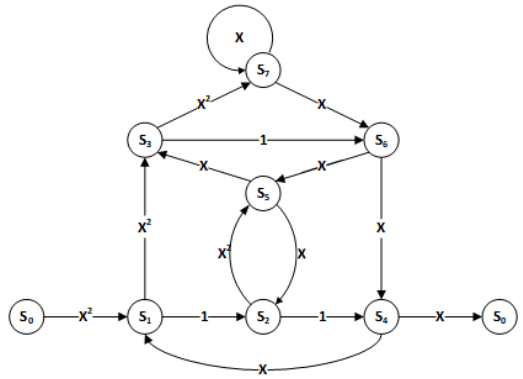

***Fig. 10**. Modified State diagram for (2, 1, 3) encoder with polynomial (13, 17)*

The state S_0 is split into initial and final state, the zero weight branch in S_0 is deleted. Each branch is illustrated with a branch gain Xd where d is the weight of the encoded bits on that branch. The parameter required to study the structure property of an encoder is listed in the Table 5 and 6.

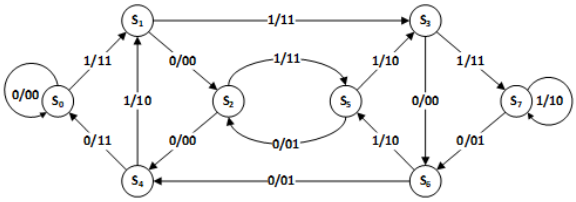

***Fig. 9**. State diagram for (2, 1, 3) encoder with polynomial (13, 17)*

TABLE 5
CYCLE AND FORWARD PATH FOR AN (2, 1, 3) ENCODER WITH THE POLYNOMIAL [13, 17]

Label	Cycles Path	Gain	Label	Forward path Path	Gain	Delta (Δ)
C1	$S_1 S_3 S_7 S_6 S_5 S_2 S_4 S_1$	X^8	FP1	$S_0 S_1 S_3 S_7 S_6 S_5 S_2 S_4 S_0$	X^{12}	1
C2	$S_1 S_3 S_7 S_6 S_4 S_1$	X^3	FP2	$S_0 S_1 S_3 S_7 S_6 S_4 S_0$	X^7	$1 - X$
C3	$S_1 S_3 S_6 S_5 S_2 S_4 S_1$	X^7	FP3	$S_0 S_1 S_3 S_7 S_6 S_5 S_2 S_4 S_0$	X^{11}	$1 - X$
C4	$S_1 S_3 S_6 S_4 S_1$	X^2	FP4	$S_0 S_1 S_3 S_6 S_4 S_0$	X^6	$1 - 2X + X^2$
C5	$S_1 S_2 S_5 S_3 S_7 S_6 S_4 S_1$	X^4	FP5	$S_0 S_1 S_2 S_5 S_3 S_7 S_6 S_4 S_0$	X^8	1
C6	$S_1 S_2 S_5 S_3 S_6 S_4 S_1$	X^3	FP6	$S_0 S_1 S_2 S_5 S_3 S_6 S_4 S_0$	X^7	$1 - X$
C7	$S_1 S_2 S_4 S_1$	X^3	FP7	$S_0 S_1 S_2 S_4 S_0$	X^7	$1 - X - X^4$
C8	$S_2 S_5 S_2$	X				
C9	$S_3 S_7 S_6 S_5 S_3$	X^5				
C10	$S_3 S_6 S_5 S_3$	X^4				
C11	$S_7 S_7$	X				

TABLE 6

CI, CIJ FOR AN (2, 1, 3) ENCODER WITH THE POLYNOMIAL [13, 17]

C_i		C_{ij},	
Label	**Gain**	**Label**	**Gain**
C2, C8	X^4	C4, C8, C11	X^4
C3, C11	X^8	C7, C10, C11	X^8
C4, C8	X^3		
C4, C11	X^3		
C6, C11	X^4		
C7, C9	X^8		
C7, C10	X^7		
C7, C11	X^4		
C8, C11	X^2		
C10, C11	X^5		

Using the equation 1, table 5 and 6, Weight Enumerated Function for the polynomial (13, 17) is as shown in the equation 8.

$$A(X) = \frac{X^6 + X^7 + X^8}{1 - 2X - X^3} = X^6 + 3X^7 + 5X^8 + ... \quad (8)$$

The above equation gives a complete description of the encoder. It concludes that the encoder has one codeword of weight 6, 3 codeword of weight 7 and 5 codeword of weight 8 and so on.

dfree = 6, Adfree = 1 and

$$\gamma = 10\log_{10}(R \times d_{free})$$
$$= 10\log_{10}(6/2)$$
$$= 4.77\,dB$$

For the polynomial [10, 11], the weight enumerated function and its structure property is analyzed is similar to the polynomial [13, 17]. The state diagram and modified state diagram are shown in the figure 11 and 12 respectively. The parameters calculation for structure property is listed in the table 7 and 8.

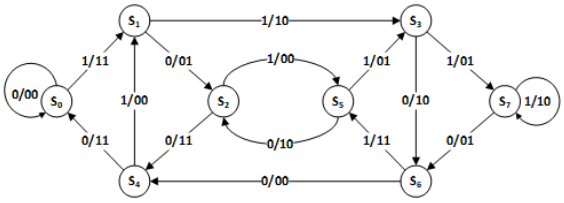

Fig. 11*. State diagram for (2, 1, 3) encoder with polynomial (10, 11)*

Weight Enumerated Function for the polynomial (10, 11) is as below

$$A(X) = \frac{X^{12} + 3X^{10} + 3X^8}{1 - X - X^2} = X^{12} + X^{11} + X^{10} + ... \quad (9)$$

dfree = 12, Adfree = 1 and

$$\gamma = 10\log_{10}(R \times d_{free})$$
$$= 10\log_{10}(12/2)$$
$$= 7.78\,dB$$

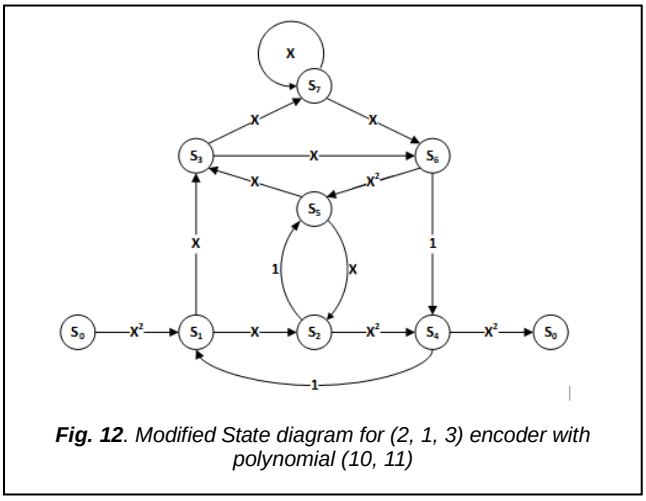

Fig. 12*. Modified State diagram for (2, 1, 3) encoder with polynomial (10, 11)*

TABLE 7

CYCLE AND FORWARD PATH FOR AN (2, 1, 3) ENCODER WITH THE POLYNOMIAL [10, 11]

Cycles			Forward path			
Label	**Path**	**Gain**	**Label**	**Path**	**Gain**	**Delta (Δ)**
C1	$S_1 S_3 S_7 S_6 S_5 S_2 S_4 S_1$	X^8	FP1	$S_0 S_1 S_3 S_7 S_6 S_5 S_2 S_4 S_0$	X^{10}	1
C2	$S_1 S_3 S_7 S_6 S_4 S_1$	X^7	FP2	$S_0 S_1 S_3 S_7 S_6 S_4 S_0$	X^9	$1 - X^3$
C3	$S_1 S_3 S_6 S_5 S_2 S_4 S_1$	X^5	FP3	$S_0 S_1 S_3 S_7 S_6 S_5 S_2 S_4 S_0$	X^7	$1 - X$
C4	$S_1 S_3 S_6 S_4 S_1$	X^4	FP4	$S_0 S_1 S_3 S_6 S_4 S_0$	X^6	$1-X-X^3+X^4$
C5	$S_1 S_2 S_5 S_3 S_7 S_6 S_4 S_1$	X^8	FP5	$S_0 S_1 S_2 S_5 S_3 S_7 S_6 S_4 S_0$	X^{10}	1
C6	$S_1 S_2 S_5 S_3 S_6 S_4 S_1$	X^5	FP6	$S_0 S_1 S_2 S_5 S_3 S_6 S_4 S_0$	X^7	$1 - X$
C7	$S_1 S_2 S_4 S_1$	X	FP7	$S_0 S_1 S_2 S_4 S_0$	X^3	$1-X-X^2+X^3-X^5$
C8	$S_2 S_5 S_2$	X^3				
C9	$S_3 S_7 S_6 S_5 S_3$	X^5				
C10	$S_3 S_6 S_5 S_3$	X^2				
C11	$S_7 S_7$	X				

TABLE 8

CI, CIJ FOR AN (2, 1, 3) ENCODER WITH THE POLYNOMIAL [10, 11]

C_i		C_{ij},	
Label	**Gain**	**Label**	**Gain**
C2, C8	X^{10}	C4, C8, C11	X^8
C3, C11	X^6	C7, C10, C11	X^4
C4, C8	X^7		
C4, C11	X^5		
C6, C11	X^6		
C7, C9	X^6		
C7, C10	X^3		
C7, C11	X^2		
C8, C11	X^4		
C10, C11	X^3		

4 RESULT AND DISCUSSION

From the Table 3.12, it is observed that the polynomial [10, 11] gives a coding gain of 7.78 dB with a code weight of 2. This properties are better than the polynomial [13, 17] which has the coding gain of 4.77 dB with the code weight of 4. Simulation of error coding techniques for polynomial [10, 11] is compared with the polynomial [13, 17] and it is discussed in the further chapter From the Table 3.16, it is observed that

the polynomial [1, 5] has better coding gain and least code weight compared to other polynomial. Therefore, simulation of error coding for polynomial [1, 5] is compared with the polynomial [5, 7]. Validation of the best polynomial which gives least error rate for the constraint length of 3 and 4 is carried out in two ways. In the first method, Watermark toolbox is used which is discussed in detail in the Appendix 1 and in the second method, real time experiment is carried out in the acoustic water tank setup, National Institute of Ocean Technology, Chennai. The detail description of the tank setup is discussed in the Appendix2

TABLE 4

STRUCTURE PROPERTIES FOR (2, 1, 3) ENCODER FOR CONSTRAINT LENGTH OF 3

Polynomial	d_{free}	A_{dfree}	γ (dB)	Code Weight	Hamming Distance
[1, 5]	3	1	3.98	2	1
[5, 7]	5	1	3.01	3	1
[3, 7]	4	1	1.76	3	1
[4, 5]	3	1	1.76	2	1
[6, 7]	4	1	3.01	3	1

TABLE 10

STRUCTURE PROPERTIES FOR (2, 1, 3) ENCODER FOR CONSTRAINT LENGTH OF 4

polynomial	d_{free}	A_{dfree}	γ (dB)	Code Weight	Hamming Distance
[13, 17]	6	1	4.77	4	1
[10, 11]	12	1	7.78	2	1
[11, 13]	8	1	6.02	3	1
[12, 13]	12	1	7.78	3	1
[14, 15]	12	1	7.78	3	1
[15, 17]	12	1	7.78	4	1
[16, 17]	12	1	7.78	4	1

REFERENCES

[1] Robert J. Urick, “Principles of Underwater Sound for Engineers”, McGraw-Hill, Third Edition, 2013.

[2] Yongjune Kim, Il Suek Koh and Yongshik Lee, “Path-loss prediction based on FDTD method and normal mode theory for underwater acoustic channel”, OCEANS'11 MTS - IEEE Kona, on Sep. 19-22. pp.1-6, 2011.

[3] Xu Zhi-Bin and Lin Xue-Yuan, “Modeling Study of Hydro-acoustic Channel Based on Ray Model”, Third International Conference on Information and Computing on July 23, Wuxi China, Vol. No: 3, pp.217-220, 2010.

[4] Francois-Xavier Socheleau, Christophe Laot and Jean-Michel Passerieux, “Stochastic replay of non-WSSUS underwater acoustic communication channels recorded at sea”, IEEE Transactions on Signal Processing, Vol. No: 59(10), pp.4838-4849, 2011.

[5] Chantri Polprasert, James A. Ritcey and Milica Stojanovic, “Capacity of OFDM systems over fading underwater acoustic channels”, IEEE Journal of Oceanic Engineering, Vol. No: 36(4), pp.514-524, 2011.

[6] Jun Won Choi, Thomas J. Riedl, Kyeongyeon Kim, Andrew C. Singer and James C. Preisig, “Practical application of turbo equalization to underwater acoustic communications”, 7th International Symposium on Wireless Communication Systems on Nov. 09, pp. 601-605, 2010.

[7] Shah C.P, Tsimenidis C.C, Sharif B.S and Neasham J. A, “EXIT chart analysis of BICM-ID based receiver for shallow underwater acoustic communications”, 7th International Symposium on Wireless Communication Systems on Nov. 09, pp. 6-10, 2010.

[8] Patricia Ceballos Carrascosa and Milica Stojanovic, “Adaptive channel estimation and data detection for underwater acoustic MIMO–OFDM systems”, IEEE Journal of Oceanic Engineering, Vol. No: 35(3), pp.635-646, 2010.

[9] Andreja Radosevic, Rameez Ahmed, Tolga M. Duman, John G. Proakis and Milica Stojanovic , “Adaptive OFDM modulation for underwater acoustic communications: design considerations and experimental results”, IEEE Journal of Oceanic Engineering, Vol. No: 39(2), pp.357-370, 2014.

[10] Yuriy V. Zakharov and Andrey K. Morozov, “OFDM transmission without guard interval in fast-varying underwater acoustic channels”, IEEE Journal of Oceanic Engineering, Vol. No: 40(1), pp.144-158, 2015.

[11] Menglu Xia, Daniel Rouseff, James A. Ritcey, Xiang Zou, Chantri Polprasert and Wen Xu, “Underwater acoustic communication in a highly refractive environment using SC–FDE”, IEEE Journal of Oceanic Engineering, Vol. No: 39(3), pp.491-499, 2014.

[12] Kai Tu, Tolga M. Duman, Milica Stojanovic and John G. Proakis,”Multiple-resampling receiver design for OFDM over doppler-distorted underwater acoustic channels”, IEEE Journal of Oceanic Engineering, Vol. No: 38(2), pp.333-346, 2013.

[13] Jian Dang, Fengzhong Qu, Zaichen Zhang and Liuqing Yang, “OFDM-IDMA communications over underwater acoustic channels”, Military Communications Conference (MILCOM) on Nov. 7-10, pp. 418-423, 2011.

[14] Tadashi Ebihara and Koichi Mizutani, “Underwater acoustic communication with a orthogonal signal division multiplexing scheme in doubly spread channels”, IEEE Journal of Oceanic Engineering, Vol. No: 39(1), pp.47-58, 2014.

[15] Samar Kaddouri, Pierre-Philippe J. Beaujean, Pierre-Jean Bouvet and Gaultier Real, “Least square and trended Doppler estimation in fading channel for high-frequency underwater acoustic communications”, IEEE Journal of Oceanic Engineering, Vol. No: 39(1), pp.179-188, 2014.

[16] Chengbing He, Siyu Huo, Qunfei Zhang, Han Wang and Jianguo Huang, “Multi-channel iterative FDE for single carrier block transmission over underwater acoustic channels” China Communications, Vol. No: 12(8), pp.55-61, 2015.

[17] Jun Tao, Yahong Rosa Zheng, Chengshan Xiao and T. C. Yang, “Robust MIMO underwater acoustic communications using turbo block decision-feedback equalization”, IEEE Journal of Oceanic

Engineering, Vol. No: 35(4), pp.948-960, 2010.
[18] Xiaohui Zhong, Fangjiong Cheny, Fei Ji and Hua Yu, “Variable step size least symbol error rate adaptive decision feedback turbo equalization for underwater channel”, OCEANS-MTS/IEEE Washington on Oct. 19-22, pp.1-4, 2016.
[19] Yanbo Wu, Min Zhu and Xinguo Lit, “Sparse linear equalizers for turbo equalizations in underwater acoustic communication”, OCEANS - MTS/IEEE Washington on Oct. 19-22, pp.1-6, 2015.
[20] Weimin Duan and Yahong Rosa Zheng, “Soft direct-adaptive turbo equalization for MIMO underwater acoustic communications”, OCEANS - MTS/IEEE Washington on Oct. 19-22, pp.1-6, 2015.
[21] Taehyuk Kang and Ronald A. Iltis, “Matching Pursuits channel estimation for an underwater acoustic OFDM modem”, IEEE International Conference on Acoustics, Speech and Signal Processing on March 31–April 4, pp.5296-5299, 2008.
[22] Longbao Wang, Jun Tao, Chengshan Xiao and Yang T. C, “Frequency-domain turbo detection for LDPC-coded single-carrier MIMO underwater acoustic communications”, OCEANS MTS-IEEE Seattle on Sep. 20-32, pp.1-5, 2010.